This paper is published as part of a *PCCP* themed issue series on biophysics and biophysical chemistry:

Biomolecular Structures: From Isolated Molecules to Living Cells

Guest Editors: Seong Keun Kim, Jean-Pierre Schermann and Taekjip Ha

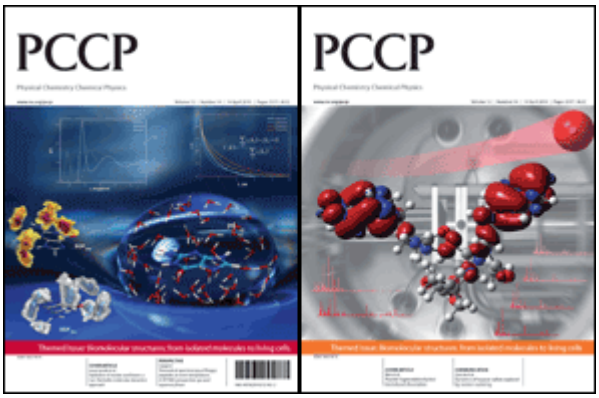

Editorial

Biomolecular Structures: From Isolated Molecules to the Cell Crowded Medium
Seong Keun Kim, Jean-Pierre Schermann, Taekjip Ha, *Phys. Chem. Chem. Phys.*, 2010
DOI: 10.1039/c004156b

Perspectives

Theoretical spectroscopy of floppy peptides at room temperature. A DFTMD perspective: gas and aqueous phase
Marie-Pierre Gaigeot, *Phys. Chem. Chem. Phys.*, 2010
DOI: 10.1039/b924048a

Communications

Dynamics of heparan sulfate explored by neutron scattering
Marion Jasnin, Lambert van Eijck, Michael Marek Koza, Judith Peters, Cédric Laguri, Hugues Lortat-Jacob and Giuseppe Zaccai, *Phys. Chem. Chem. Phys.*, 2010
DOI: 10.1039/b923878f

Papers

Infrared multiple photon dissociation spectroscopy of cationized methionine: effects of alkali-metal cation size on gas-phase conformation
Damon R. Carl, Theresa E. Cooper, Jos Oomens, Jeff D. Steill and P. B. Armentrout, *Phys. Chem. Chem. Phys.*, 2010
DOI: 10.1039/b919039b

Structure of the gas-phase glycine tripeptide
Dimitrios Toroz and Tanja van Mourik, *Phys. Chem. Chem. Phys.*, 2010
DOI: 10.1039/b921897a

Photodetachment of tryptophan anion: an optical probe of remote electron
Isabelle Compagnon, Abdul-Rahman Allouche, Franck Bertorelle, Rodolphe Antoine and Philippe Dugourd, *Phys. Chem. Chem. Phys.*, 2010
DOI: 10.1039/b922514p

A natural missing link between activated and downhill protein folding scenarios
Feng Liu, Caroline Maynard, Gregory Scott, Artem Melnykov, Kathleen B. Hall and Martin Gruebele, *Phys. Chem. Chem. Phys.*, 2010
DOI: 10.1039/b925033f

Vibrational signatures of metal-chelated monosaccharide epimers: gas-phase infrared spectroscopy of Rb^+-tagged glucuronic and iduronic acid
Emilio B. Cagmat, Jan Szczepanski, Wright L. Pearson, David H. Powell, John R. Eyler and Nick C. Polfer, *Phys. Chem. Chem. Phys.*, 2010
DOI: 10.1039/b924027f

Stepwise hydration and evaporation of adenosine monophosphate nucleotide anions: a multiscale theoretical study
F. Calvo and J. Douady, *Phys. Chem. Chem. Phys.*, 2010
DOI: 10.1039/b923972c

Reference MP2/CBS and CCSD(T) quantum-chemical calculations on stacked adenine dimers. Comparison with DFT-D, MP2.5, SCS(MI)-MP2, M06-2X, CBS(SCS-D) and force field descriptions
Claudio A. Morgado, Petr Jurečka, Daniel Svozil, Pavel Hobza and Jiří Šponer, *Phys. Chem. Chem. Phys.*, 2010
DOI: 10.1039/b924461a

Photoelectron spectroscopy of homogeneous nucleic acid base dimer anions
Yeon Jae Ko, Haopeng Wang, Rui Cao, Dunja Radisic, Soren N. Eustis, Sarah T. Stokes, Svetlana Lyapustina, Shan Xi Tian and Kit H. Bowen, *Phys. Chem. Chem. Phys.*, 2010
DOI: 10.1039/b924950h

Sugar–salt and sugar–salt–water complexes: structure and dynamics of glucose–KNO_3–$(H_2O)_n$
Madeleine Pincu, Brina Brauer, Robert Benny Gerber and Victoria Buch, *Phys. Chem. Chem. Phys.*, 2010
DOI: 10.1039/b925797g

Hydration of nucleic acid bases: a Car–Parrinello molecular dynamics approach
Alona Furmanchuk, Olexandr Isayev, Oleg V. Shishkin, Leonid Gorb and Jerzy Leszczynski, *Phys. Chem. Chem. Phys.*, 2010
DOI: 10.1039/b923930h

Conformations and vibrational spectra of a model tripeptide: change of secondary structure upon micro-solvation
Hui Zhu, Martine Blom, Isabel Compagnon, Anouk M. Rijs, Santanu Roy, Gert von Helden and Burkhard Schmidt, *Phys. Chem. Chem. Phys.*, 2010
DOI: 10.1039/b926413b

Peptide fragmentation by keV ion-induced dissociation
Sadia Bari, Ronnie Hoekstra and Thomas Schlathölter, *Phys. Chem. Chem. Phys.*, 2010
DOI: 10.1039/b924145k

Structural, energetic and dynamical properties of sodiated oligoglycines: relevance of a polarizable force field
David Semrouni, Gilles Ohanessian and Carine Clavaguéra, *Phys. Chem. Chem. Phys.*, 2010
DOI: 10.1039/b924317h

Studying the stoichiometries of membrane proteins by mass spectrometry: microbial rhodopsins and a potassium ion channel
Jan Hoffmann, Lubica Aslimovska, Christian Bamann, Clemens Glaubitz, Ernst Bamberg and Bernd Brutschy, *Phys. Chem. Chem. Phys.*, 2010
DOI: 10.1039/b924630d

Sub-microsecond photodissociation pathways of gas phase adenosine 5′-monophosphate nucleotide ions
G. Aravind, R. Antoine, B. Klærke, J. Lemoine, A. Racaud, D. B. Rahbek, J. Rajput, P. Dugourd and L. H. Andersen, *Phys. Chem. Chem. Phys.*, 2010
DOI: 10.1039/b921038e

DFT-MD and vibrational anharmonicities of a phosphorylated amino acid. Success and failure
Alvaro Cimas and Marie-Pierre Gaigeot, *Phys. Chem. Chem. Phys.*, 2010
DOI: 10.1039/b924025j

Infrared vibrational spectra as a structural probe of gaseous ions formed by caffeine and theophylline
Richard A. Marta, Ronghu Wu, Kris R. Eldridge, Jonathan K. Martens and Terry B. McMahon, *Phys. Chem. Chem. Phys.*, 2010
DOI: 10.1039/b921102k

Laser spectroscopic study on (dibenzo-24-crown-8-ether)–water and –methanol complexes in supersonic jets
Satoshi Kokubu, Ryoji Kusaka, Yoshiya Inokuchi, Takeharu Haino and Takayuki Ebata, *Phys. Chem. Chem. Phys.*, 2010
DOI: 10.1039/b924822f

Macromolecular crowding induces polypeptide compaction and decreases folding cooperativity
Douglas Tsao and Nikolay V. Dokholyan, *Phys. Chem. Chem. Phys.*, 2010
DOI: 10.1039/b924236h

Electronic coupling between cytosine bases in DNA single strands and *i*-motifs revealed from synchrotron radiation circular dichroism experiments
Anne I. S. Holm, Lisbeth M. Nielsen, Bern Kohler, Søren Vrønning Hoffmann and Steen Brøndsted Nielsen, *Phys. Chem. Chem. Phys.*, 2010
DOI: 10.1039/b924076d

Photoionization of 2-pyridone and 2-hydroxypyridine
J. C. Poully, J. P. Schermann, N. Nieuwjaer, F. Lecomte, G. Grégoire, C. Desfrançois, G. A. Garcia, L. Nahon, D. Nandi, L. Poisson and M. Hochlaf, *Phys. Chem. Chem. Phys.*, 2010
DOI: 10.1039/b923630a

Insulin dimer dissociation and unfolding revealed by amide I two-dimensional infrared spectroscopy
Ziad Ganim, Kevin C. Jones and Andrei Tokmakoff, *Phys. Chem. Chem. Phys.*, 2010
DOI: 10.1039/b923515a

Six conformers of neutral aspartic acid identified in the gas phase
M. Eugenia Sanz, Juan C. López and José L. Alonso, *Phys. Chem. Chem. Phys.*, 2010
DOI: 10.1039/b926520a

Binding a heparin derived disaccharide to defensin inspired peptides: insights to antimicrobial inhibition from gas-phase measurements
Bryan J. McCullough, Jason M. Kalapothakis, Wutharath Chin, Karen Taylor, David J. Clarke, Hayden Eastwood, Dominic Campopiano, Derek MacMillan, Julia Dorin and Perdita E. Barran, *Phys. Chem. Chem. Phys.*, 2010
DOI: 10.1039/b923784d

Guanine–aspartic acid interactions probed with IR–UV resonance spectroscopy
Bridgit O. Crews, Ali Abo-Riziq, Kristýna Pluháčková, Patrina Thompson, Glake Hill, Pavel Hobza and Mattanjah S. de Vries, *Phys. Chem. Chem. Phys.*, 2010
DOI: 10.1039/b925340h

Investigations of the water clusters of the protected amino acid Ac-Phe-OMe by applying IR/UV double resonance spectroscopy: microsolvation of the backbone
Holger Fricke, Kirsten Schwing, Andreas Gerlach, Claus Unterberg and Markus Gerhards, *Phys. Chem. Chem. Phys.*, 2010
DOI: 10.1039/c000424c

Probing the specific interactions and structures of gas-phase vancomycin antibiotics with cell-wall precursor through IRMPD spectroscopy
Jean Christophe Poully, Frédéric Lecomte, Nicolas Nieuwjaer, Bruno Manil, Jean Pierre Schermann, Charles Desfrançois, Florent Calvo and Gilles Grégoire, *Phys. Chem. Chem. Phys.*, 2010
DOI: 10.1039/b923787a

Two-dimensional network stability of nucleobases and amino acids on graphite under ambient conditions: adenine, L-serine and L-tyrosine
Ilko Bald, Sigrid Weigelt, Xiaojing Ma, Pengyang Xie, Ramesh Subramani, Mingdong Dong, Chen Wang, Wael Mamdouh, Jianguo Wang and Flemming Besenbacher, *Phys. Chem. Chem. Phys.*, 2010
DOI: 10.1039/b924098e

Importance of loop dynamics in the neocarzinostatin chromophore binding and release mechanisms
Bing Wang and Kenneth M. Merz Jr., *Phys. Chem. Chem. Phys.*, 2010
DOI: 10.1039/b924951f

Structural diversity of dimers of the Alzheimer Amyloid-(25-35) peptide and polymorphism of the resulting fibrils
Joan-Emma Shea, Andrew I. Jewett, Guanghong Wei, *Phys. Chem. Chem. Phys.*, 2010
DOI: 10.1039/c000755m

Conformations and vibrational spectra of a model tripeptide: change of secondary structure upon micro-solvation†

Hui Zhu,*[a] Martine Blom,[b] Isabel Compagnon,[b] Anouk M. Rijs,[b] Santanu Roy,[c] Gert von Helden*[d] and Burkhard Schmidt*[a]

Received 15th December 2009, Accepted 29th January 2010
First published as an Advance Article on the web 23rd February 2010
DOI: 10.1039/b926413b

Mid-infrared (IR) hole burning spectra of the model tripeptide Z-Aib-Pro-NHMe (Z = benzyloxycarbonyl) in gas phase and its micro-clusters with one and two methanol molecules are presented. To establish a relation between experimental spectra and the underlying conformations, calculations at the DFT [B3LYP/6-311++G(d,p)] level of theory are performed. In particular, the intra-peptide and the peptide–methanol hydrogen bonds can be identified from spectral shifts in the amide I, II, and III regions. While the unsolvated tripeptide as well as its one-methanol cluster prefer a γ-turn structure, a β-turn structure is found for the two-methanol cluster, in agreement with previous condensed phase studies. Comparison of measured and simulated spectra reveals that the favorable methanol binding sites are at the head and tail parts of the tripeptide. The interconversions between γ-turn and β-turn structures are governed by potential barriers below 10 kJ mol^{-1} inside one of the low energy basins of the potential energy surface.

I. Introduction

The structure and function of biological molecules are determined by a subtle interplay between various intra- and intermolecular interactions. One of the challenges in molecular biophysics is to disentangle those interactions to obtain a better and more fundamental insight into the key factors determining their dynamics, and measuring the properties of molecules as a function of environment can add important contributions to this goal. For most biological molecules, the aqueous solution phase is the natural environment and many experimental techniques exist to investigate dissolved molecules. However, molecules can also be studied "naked" in the gas phase, where only the intramolecular interactions are present, thus offering a unique possibility to study the intrinsic properties of molecules. The gas phase can also offer well controlled conditions as mass spectrometric techniques allow full control over the exact composition and aggregation state of the molecules. Further, investigations in the gas phase allow experiments to be performed at low temperatures down to the (sub) Kelvin range without having complications due to interferences with matrices, as one would have in the condensed phase. This becomes important when performing spectroscopic experiments, as the low temperature allows for the measurement of spectra at much higher resolution, compared to room temperature.

The structures of peptides and proteins will usually differ in the gas phase and in the condensed phase. Those differences will be most dramatic when electrostatic intra- and intermolecular interactions are prominent. However, also in cases where hydrogen bonding (H-bonding) is the dominant interaction, the competition between intramolecular H-bonding and H-bonding to the solvent will have a decisive influence on the structure. This will be especially the case when different intramolecular structural motifs are nearly isoenergetic, where the addition of only a few solvent molecules can drastically alter the structure. It is thus of general interest to map the transition from the isolated molecule in the gas phase, *via* the molecule interacting with only a few solvent molecules to the molecule in its native environment. Several studies focused on the structures of amino acids solvent complexes and specifically on the question of how hydration determines the internal charge distribution of gas-phase biological molecules having both basic and acidic sites.[1–6] In other studies, the structural implications of solvent addition to nucleobases[7] or saccharides[8,9] as well as the proton dynamics in complexes of organic molecules with water[10,11] were investigated.

We here report on the structure of the doubly terminated tripeptide Z-Aib-Pro-NHMe (Z = benzyloxycarbonyl), solvent free in the gas phase, as well as complexed with one and two methanol molecules, see Fig. 1. The Aib-Pro sequence is of importance for the structure of several natural and

[a] *Institut für Mathematik, Freie Universität Berlin, Arnimallee 6, D-14195 Berlin, Germany. E-mail: hui.zhu@fu-berlin.de, burkhard.schmidt@fu-berlin.de*
[b] *FOM Institute for Plasma Physics Rijnhuizen, Edisonbaan 14, NL-3439 Nieuwegein, The Netherlands*
[c] *Center for Theoretical Physics and Zernike Institute for Advanced Materials, University of Groningen, Nijenborgh 4, Groningen NL-9747 AG, The Netherlands*
[d] *Fritz Haber Institut der Max-Planck-Gesellschaft, Faradayweg 4-6, D-14195 Berlin, Germany. E-mail: helden@fhi-berlin.mpg.de*

† Electronic supplementary information (ESI) available: Minimum energy conformations for Z-Aib-Pro-NHMe peptide from DFT calculations [B3LYP/6-311++G(d,p)] (Table S1); transition states connecting the conformations for Z-Aib-Pro-NHMe peptide (Table S2); minimum energy conformations of Z-Aib-Pro-NHMe clusters with one methanol molecule from DFT calculations [B3LYP/6-311++G(d,p)] (Table S3); same as Table S3, but for Z-Aib-Pro-NHMe clusters with two methanol molecules (Table S4). See DOI: 10.1039/b926413b

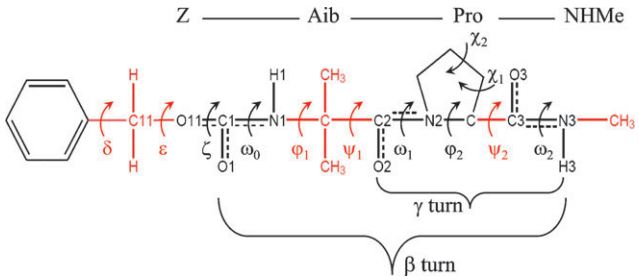

Fig. 1 Skeletal structure of Z-Aib-Pro-NHMe peptide. Arrows indicate twelve dihedral angles along the backbone used to characterize the backbone conformations. Black color: rigid parts. Red color: flexible parts.

synthetic peptides. Aib-Pro containing sequences are also of considerable pharmaceutical interest as they introduce turns in peptidic chains and can be used as β-sheet breakers.[12–22] The rare amino acid α-aminoisobutyric acid (Aib) naturally occurs in some antibiotic peptides. Its two methyl groups on the α-carbon introduce considerable steric constraints and cause a strong propensity to form turns or helices structures. The amino acid proline (Pro) contains a pyrrolidine ring that reduces the N–C_α backbone torsional flexibility and is often found in β- and γ-turn structures. Further, it reduces the ability to form H-bonds, as it lacks the N–H group. Moreover the pyrrolidine ring can adopt two near-degenerate conformations, *i.e.*, the up and down ring-puckering.[23–29] In Z-Aib-Pro-NHMe, the secondary structure is governed by two competing intramolecular H-bonds, one that forms a tight seven-membered-ring (C_7-ring) with a γ-turn and one that causes a wider C_{10}-ring with a β-turn.[30–32] In the condensed phase, several studies show that a β-turn structure is apparently preferred[19,20] while in the gas phase, a γ-turn structure is formed.[14] Calculations indicate that for isolated species, those two structural motifs are nearly isoenergetic[14] and it would be of interest to observe how addition of individual solvent molecules influences the structural preferences.

To study biomolecules in the gas phase, molecular beam methods combined with optical spectroscopy can be used. Especially IR-UV holeburning techniques[33] are powerful, as they allow for spectroscopy on mass- and conformer-selected, jet-cooled molecules. Consequently, it has been applied to peptide molecules both in the 3 μm X–H stretching[34–43] as well as in the fingerprinting region above 5 μm.[14,35,39,43–47] Here we present experimental mid IR spectra of gas-phase Z-Aib-Pro-NHMe without solvent as well as with one or two methanol molecules attached. The experimental spectra are compared to theoretical predictions, which provides detailed information on both the secondary structure of the peptide as well as the site of attachment of the methanol molecules. Such a comparison can then be used to test our understanding and the experimental data can serve as a calibration for theory.

II. Experimental and computational details

A. Experimental setup

The synthesis of Z-Aib-Pro-NHMe as well as the experimental procedure to obtain its gas phase mid-IR spectrum have been described previously[14] and only a brief outline as well as experimental differences will be given here. To obtain the infrared (IR) absorption spectra of isolated, internally cooled Z-Aib-Pro-NHMe, a pulsed molecular beam set-up combined with a laser desorption source and a time-of-flight mass spectrometer is used.[48,49] The sample is mixed with some graphite powder and deposited on a graphite sample bar. This translatable sample bar is placed directly under the nozzle opening of the pulsed valve, which has a diameter of 0.5 mm and is operating at 10 Hz. Z-Aib-Pro-NHMe is brought into the gas phase by laser desorption using a ~3 mJ pulse at 1064 nm, and cooled down in a supersonic molecular beam expansion of argon with a backing pressure of 3 bar. Additionally, the Z-Aib-Pro-NHMe···MeOH clusters are formed in a methanol-moisturized supersonic argon expansion. The neutral molecular beam is skimmed and intersected perpendicularly with a tunable UV laser beam (frequency doubled output of a YAG-pumped dye laser) operating at 10 Hz to ionize the molecules. The ions are accelerated into the time-of-flight tube and detected at the microchannel plate detector.

To obtain the IR absorption spectra of isolated, gas-phase Z-Aib-Pro-NHMe and its methanol clusters, IR-UV ion-dip spectroscopy was used.[5,48,50] Ions are constantly produced from ground state molecules using a 2-photon resonant ionization scheme. While the UV spectrum of the bare peptide shows some structure and two conformers can be selectively excited at two UV frequencies (37 492 cm^{-1} and 37 448 cm^{-1}),[14] no structure is observed in the UV spectra of the clusters with one and two methanol molecules, and excitation is performed at a single frequency of 37 504 cm^{-1}. Prior to passing this UV beam, the molecules are excited with the IR laser. If the IR laser is resonant with a vibrational transition, molecular population is transferred from the ground state into a vibrationally excited state, resulting in a depletion of the ground state population and thus a dip in the ion signal. By measuring the ion yield of the mass of interest, while scanning the wavelength of the IR laser, the IR ion-dip spectrum is obtained.

The IR absorption in the amide I, II, and III and fingerprint region (below 1500 cm^{-1}) was recorded at the free electron laser facility (FELIX) at the FOM Institute for Plasma Physics Rijnhuizen.[51] FELIX produces pulses of about 5 μs length with pulse energies of about 100 mJ and a spectral line width of typically 0.5–1% FWHM (~10 cm^{-1}) in the scanned region. The IR laser beam is aligned perpendicularly to the molecular beam and counter propagating to the slightly focused UV laser beam. In these experiments, the molecular beam and the UV laser are running at 10 Hz, while FELIX is operating at 5 Hz. By recording separately (alternating) both the IR-on and IR-off signals, a normalized ion-dip spectrum is obtained in order to minimize the signal fluctuations due to long-term drifts in the UV laser power or source conditions. Furthermore, the spectra are corrected for the intensity variations of the IR light over the complete scanning range.

B. Calculations of structures and spectra

Density functional theory (DFT) calculations are carried out for the bare Z-Aib-Pro-NHMe tripeptide and its clusters with

one or two methanol molecules. The computations are based on Becke's three-parameter exchange functional[52] along with the Lee–Yang–Parr correlation functional (B3LYP)[53] as implemented in the GAUSSIAN 03 program suite.[54] The standard 6-311++G(d,p) split-valence basis with both polarization and diffuse functions[55–57] is chosen for the singlet ground-state geometry optimization and frequency calculations. This leads to 725 basis functions for the peptide and additional 72 basis functions for each methanol molecule. The fully optimized stationary points are further characterized by harmonic vibrational frequency analysis to verify whether they are minima with all frequencies being real or first order saddle points with only one imaginary frequency. The zero-point energy (ZPE) corrections to the total energies are obtained from the calculated vibrational frequencies. Note that the ZPE corrections rarely affect the order of the relative energies. The use of modern DFT methods for the computations of different properties of molecules of biological importance has been overall appreciated.[58,59] While sometimes DFT methods are suffering from certain deficiencies,[11] vibrational spectra obtained from DFT/B3LYP calculations are known to often agree very well with experimental spectra within the mid-IR region (500–1800 cm^{-1}) for systems where intra- and intermolecular H-bonding are the dominant, non-covalent interactions.[5,14,60–62] Throughout this work, all calculated frequencies are scaled with a common factor of 0.983 to match our experiments. The vibrational frequencies have been convoluted with Gaussian bell curves of 15.5 cm^{-1} FWHM.

III. Results and discussion

A. Bare peptide conformers

As shown in Fig. 1, the skeletal structure of the model peptide is mainly described by 12 dihedral angles δ, ε, ζ, ω_0, ϕ_1, ψ_1, ω_1, ϕ_2, ψ_2, ω_2, χ_1, χ_2, given in degrees throughout this work. The DFT values for the optimized torsional angles of various conformers of the bare Z-Aib-Pro-NHMe tripeptide are listed in Table 1. The rigid parts of the structures of the tripeptide are mainly the benzene ring and the three peptide groups (Z-Aib, Aib-Pro and Pro-NHMe). While the Pro-NHMe peptide group is of canonical form, in the Aib-Pro the H atom is substituted by the alkyl group forming the five-membered pyrrolidine ring that essentially restricts the dihedral angle in a small range $-90 < \phi_2 < -72$. The pyrrolidine ring can adopt two puckering structures as indicated by Fig. 2(c). Up-puckering (U) is characterized by $-37 < \chi_1 < -7$ and $18 < \chi_2 < 48$, while down-puckering (D) is found at $11 < \chi_1 < 41$ and $-48 < \chi_2 < -18$.[26] In contrast to usual peptide bonds, the C(1)═O(1) of the Z-Aib peptide group is linked to the O(11) atom thus forming an extended four-centered π system with the C(11)–O(11)–C(1) angle of ~117 being close to that expected for an sp2 hybridization of the O(11) atom. That atom can donate π-electron density thus slightly enhancing the double-bond nature of C(1)═O(1) bond while reducing the double-bond nature of C(1)–N(1) bond. As a result, the C(1)–O(11) single bond adjacent to Z-Aib peptide bond shows some double-bond nature and can adopt either $\zeta = 180$ or $\zeta = 0$ conformations as confirmed by our DFT-calculations.

The five dihedral angles δ, ε, ϕ_1, ψ_1, and ψ_2 describe the relatively flexible torsions about single-bonds leading to a rather large conformational space of the chosen model tripeptide Z-Aib-Pro-NHMe. It can adopt two types of turn structures, namely γ- and β-turns. The dihedral angles and energies of energetically low-lying turn structures are listed in

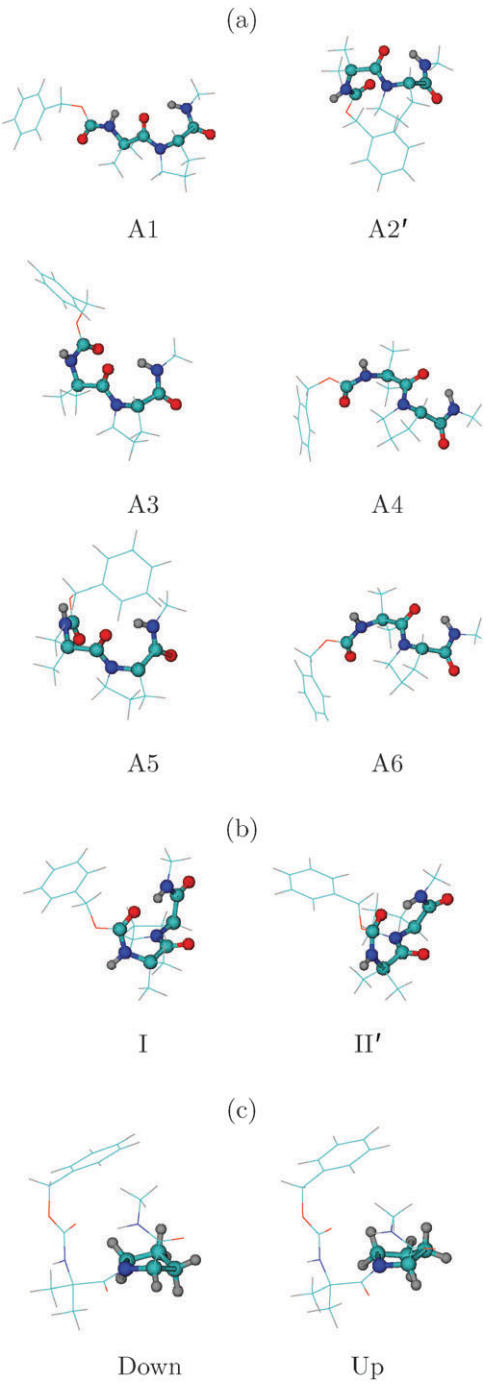

Fig. 2 Minimum energy structures of bare Z-Aib-Pro-NHMe peptide. (a) Inverse γ-turn structures with different Aib orientations. (b) Two types of β-turn structures. (c) Pyrrolidine-ring down- and up-puckering.

Table 1 Minimum energy conformations for Z-Aib-Pro-NHMe peptide from DFT calculations [B3LYP/6-311++G(d,p)]: dihedral angles (in degrees), relative energies without and with zero point energies (in kJ mol^{-1}). A*n* and B*n* (n = 1,2,2′,…, indicating different Aib orientations) are all *trans* and *cis* (Z-Aib) conformations of γ turn structures, respectively. I and II′ are β turn structures. a,b,… are different Z-cap orientations. U,D indicate up- and down puckering of the Pro ring. For more minimum energy structures as well as saddle point structures, see ESI†

Conformation	ϕ_1	ψ_1	ϕ_2	ψ_2	χ_1	χ_2	DFT	DFT + ZPE
A1aD	175	175	−82	77	32	−39	0.1	0.0
A1bD	176	175	−83	76	32	−40	0.0	0.1
A2bU	55	51	−84	79	−9	29	5.9	5.8
A2′bD	−57	−42	−86	75	33	−36	1.9	0.8
A2′bU	−56	−38	−80	82	−12	30	1.7	1.8
A3bD	63	−163	−87	72	34	−37	9.9	10.6
A4bD	−172	50	−82	74	34	−39	11.0	10.5
A5bD	68	−109	−82	71	35	−39	13.1	14.2
A6bD	−118	52	−81	73	32	−40	10.9	11.3
B2bU	60	53	−83	79	−10	29	9.2	9.6
B2′bU	−59	−33	−74	92	−17	34	10.4	10.0
IbD	−56	−37	−88	6	34	−37	1.9	0.9
IbU	−57	−33	−72	−14	−22	36	2.2	1.0
II′bD	53	−139	−90	12	35	−38	11.7	11.6
II′bU	56	−147	−73	−6	−26	38	15.5	14.7

Table 1 and the corresponding conformations of the backbone are shown in Fig. 2(a) and (b).

All γ-turn structures involve N(3)–H(3)···O(2)═C(2) H-bonding between neighboring peptide groups leading to formation of a C7-ring. Due to the chiral restriction induced by the Pro residue, only the inverse γ-turn is possible with the Ramachandran angles within the C7-ring being essentially fixed around $\phi_2 \approx -80$ and $\psi_2 \approx 80$. In order to form the γ-turn structure, both the Aib-Pro and Pro-NHMe peptide bonds should be in *trans*-conformation, while the Z-Aib peptide bond outside the γ-turn can adopt the favorable *trans* ($\omega_0 = 180$) or the less favorable *cis* ($\omega_0 = 0$) conformations. When combined with two possible choices for the C(1)–O(11) bond ($\zeta = 0$ or $\zeta = 180$), two low-lying structures are possible for $\zeta = 180$ and $\omega_0 = 180$ (termed A) and $\zeta = 180$ and $\omega_0 = 0$ (termed B). The combination of $\zeta = 0$ and $\omega_0 = 180$ (termed C) is about 30 kJ mol^{-1} higher than the related A conformer and shall not be discussed further. Outside the γ-turn, the orientation of the Aib residue can be described by the torsional angles ϕ_1 and ψ_1, with different orientations labeled by 1, 2, 2′, 3, 3′, 4, 4′ 5, 5′, 6, 6′ (see Fig. 2(a) and Table 1). The orientation 1 with ϕ_1 and ψ_1 close to 180 around the Aib residue shows an additional H-bond-like (N(1)–H(1)···O(2)═C(2)) C5-ring,[39,63] with the A1aD conformer being the global minimum. The orientations 2 and 2′ are similar to the respective left-handed and right-handed α-helical structures with opposite signs of ϕ_1 and ψ_1.

All β-turn structures involve N(3)–H(3)···O(1)═C(1) H-bonding between next but one peptide groups leading to formation of a C10-ring. The standard classification of the various types of β-turns is based on two neighboring pairs of Ramachandran angles [ϕ_1, ψ_1, ϕ_2, ψ_2].[30–32,64] In our calculations, two types of β-turns are found: type I and II′, with the respective of torsional angles [−57 ± 1, −35 ± 2, −80 ± 8, −4 ± 10] and [55 ± 2, −143 ± 4, −81 ± 9, 3 ± 9]. For the Z-Aib-Pro-NHMe tripeptide, type I is more stable than type II′. The reversed forms I′ and II are not found due to chiral restrictions imposed by the Pro residue. Within β-turns, all peptide bonds should be in *trans* conformation.

For both γ-turn and β-turn structures, the pyrrolidine ring can adopt up- and down-puckering structures that may affect the orientation of the Pro residue as described by the dihedral angles ϕ_2, ψ_2. As can be seen from Table 1 the puckering degree of freedom has only small effects on the ϕ_2, ψ_2 values of Pro within γ-turns, but larger effects on those within β-turns, probably because a C10-ring with three flexible torsions (ϕ_1, ψ_1, ψ_2) offers more conformational freedom than a C7-ring with only one flexible torsion (ψ_2).

Due to the weak interactions between the hydrogen atoms in the benzene ring and different oxygen atoms, 7 kinds of Z-cap orientations described by dihedral angles δ and ε are found in our calculations. They are labeled by a, b, c, e, f, g and h, see the ESI.† Since the Z-Cap orientations are essentially free and do not significantly affect the energies according to our DFT calculations, we will consider only the b-orientation as example.

B. Bare peptide mid-IR spectrum

In this section the vibrational spectra of bare Z-Aib-Pro-NHMe tripeptide in the mid-IR region are discussed. Since there are three peptide bonds with different substitutions, the related amide I, II, and III vibrational modes are mostly non-overlapping and straightforward to assign, see Fig. 3 for the low-lying A1bD conformer as example. The amide I vibrations, absorbing around 1600–1750 cm^{-1}, arise mainly from the C═O stretching vibration. Peak #2 around 1705 cm^{-1} is due to the Pro-NHMe amide I vibration which is rather close to the value of 1713 cm^{-1} for *trans* N-methyl-acetylamide (MeCO–NHMe) which is the simplest derivative with a standard peptidic bond. Peak #1 at 1725 cm^{-1} due to Z-Aib is blue-shifted, which indicates strengthening of the C(1)═O(1) bond due to the neighboring O(11) atom, whereas absorption #3 at 1616 cm^{-1} localized in Aib-Pro is red-shifted as a result of the lack of an NH group for the peptide bond and the simultaneous formation of H-bonds within the C5- and C7-rings with the O(2) atom. The amide II modes are out-of-phase combinations of N–H in-plane bending and C–N stretching vibrations. Peak #4 is essentially due to the amide II vibration of Pro-NHMe while that of the Z-Aib peptide bond is red-shifted due to the weakened C(1)–N(1) bond. Moreover, the latter is split into peaks #5 at 1498 cm^{-1} and #6 at 1468 cm^{-1}, possibly caused by the slight coupling with Aib-Pro amide I modes due to the C5-ring structure present in A1 conformations. The amide III modes are in-phase combinations of N–H bending and C–N stretching vibrations. Peak #9 around 1246 cm^{-1} is related to the amide III vibration of Z-Aib, with an unresolved low intensity feature at 1234 cm^{-1} caused by the amide III vibration of Pro-NHMe. Peaks #7 (1411 cm^{-1}) and #8 (1380/1369 cm^{-1}) between the amide II and amide III regions are related to C(2)–N(2) stretching vibrations of the Aib-Pro peptide bond. Note that they do not split into amide II or III modes due to the lack of combination of N–H bending. Finally, the highest intensity peak #10 at 1061 cm^{-1} is assigned to an

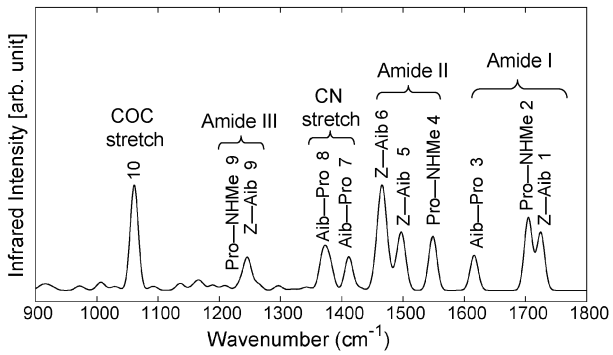

Fig. 3 Assignment of mid-IR vibrational modes of bare Z-Aib-Pro-NHMe peptide for example of all *trans* A1bD γ-turn structure.

asymmetric C–O–C stretching vibration involving the backbone O(11) atom.

Compared with the A1 conformers, other low-lying conformers such as A2, A2′ and I have different Aib orientations and their spectra exhibit a single amide II peak of the Z-Aib peptide bond around 1500 cm^{-1} (see Fig. 4). The A2′, A2, B2′, and B2 conformers show a γ-turn structure centered at the Pro residue, while the IU conformer shows a β-turn structure centered at the Aib and Pro residues. Changing from γ to β turn structures, the formation of the β-turn H-bond leads to a red-shift of the Z-Aib amide I vibration #1, while the breaking of the γ-turn H-bond leads to a blue-shift of the Aib-Pro amide I vibration #3. Hence, the β turn structure shows three closely spaced amide I peaks while γ-turn structure shows three well separated peaks, which is in agreement with experimental spectra A and B of the bare tripeptide. Thus, the experimental spectra can be unambiguously assigned to γ-turn structures. Also the up or down ring-puckering conformations can be distinguished from their spectral signatures around 1400 cm^{-1}, see Fig. 4. For the example of the A2′D and A2′U conformers, the Aib-Pro peptide bond shows single strong C–N stretching vibrations (#7) for up-puckered structure, which is split into two peaks with nearly equal intensity for down-puckered conformations, possibly due to enhanced coupling with CH bending of the pyrrolidine ring. The former intensity pattern is found for both experimental spectra of A and B, thus indicating the preference of up-puckered structures. Also the difference between all-*trans* (A) structures and *cis* Z-Aib (B) structures ($\omega_0 \sim 0$) has a clear signature in mid-IR spectra, see Fig. 4. In spectra of A conformations, the peak around 1500 cm^{-1} resulting from Z-Aib amide II vibrations, disappears in the spectra of B conformation. Furthermore, the intensity of peak #9 at 1230 cm^{-1} is reduced in the spectra of B conformations. Instead, strongly absorbing modes appear around 1300$\cdots$1320 cm^{-1} which correspond to in phase combination of C–N stretching and N–H bending vibrations. Furthermore, the intensity of the Z-Aib amide I spectrum (#1) increases when going from A to B structures. For the smaller MeCO-NHMe model system, the same changes are described in ref. 65. These drastic changes are indeed found to be the major differences between the experimental spectra A and B, thus indicating the coexistence of all-*trans* and *cis* Z-Aib ($\omega_0 \sim 0$) conformations under the conditions of our molecular

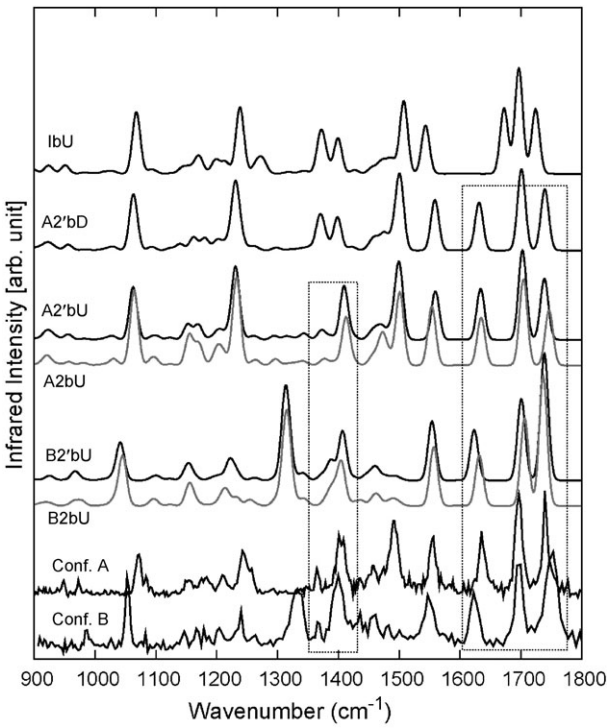

Fig. 4 Comparison of simulated and experimental mid-IR spectra of bare Z-Aib-Pro-NHMe peptide comparing β (IbU) *vs.* γ (A2′bD) turn structures, down (A2′bD) *vs.* up (A2′bU) puckering of the Pro ring, and *trans* (A2′bU) *vs. cis* (B2′bU) conformation of Z-Aib.

beam experiments. In addition, comparison of more than 10 spectra for different Aib orientations yields that experimental spectrum A (obtained at UV frequency 37 492 cm^{-1}) can be assigned to either A2′U or A2U while experimental spectrum B (37 448 cm^{-1}) resembles most closely the spectra calculated for B2′U or B2U. Finally, it is mentioned that the effects of different Z-cap orientations on the mid-IR spectra are too small to uniquely assign certain conformations.

C. Bare peptide potential energy surface

A schematic view of the potential energy surface (PES) for the Z-Aib-Pro-NHMe tripeptide is given in Fig. 5. Only isomers in a small range of energies (~20 kJ mol^{-1}) above the global minimum A1bD are shown. The arrows indicate the interconversion pathways and the height of the corresponding

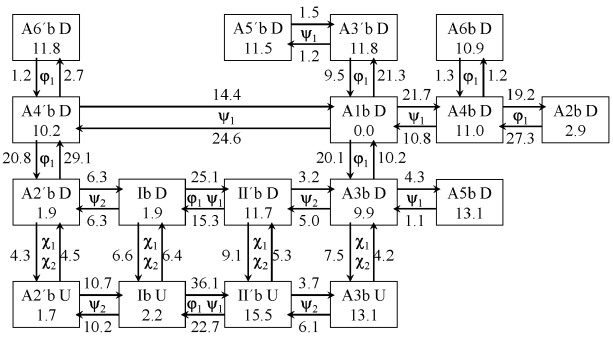

Fig. 5 Sketch of potential energy surface of bare Z-Aib-Pro-NHMe peptide: network of local minima and transition states.

transition states are given. The structural and energetic parameters of these transition states are listed in the ESI.† In each case, the corresponding transition paths involve only one or two of the flexible dihedral angles. Hence, the PES can be represented as a network in which transitions are assumed to occur step by step *via* the corresponding transition states. Several kinds of important transitions are discussed in the following.

The upper part of Fig. 5 mainly describes the conformational space spanned by the dihedral angles ϕ_1, ψ_1, ψ_2. Three low-energy regions of the PES can be generated by the rotations of ϕ_1 and ψ_1 involving relatively large barriers (20–30 kJ mol^{-1}) due to the steric hindrance from the two methyl groups (Aib) and the pyrrolidine ring structures (Pro). The lowest basin is located around the global minimum A1bD. Rotating angle ϕ_1 from $\sim$180 to $\pm$63 can bring A1bD to A3bD or A3′bD conformers, respectively, over potential barriers higher than 20 kJ mol^{-1}. Alternatively, a rotation of ψ_1 from $\sim$180 to 50 or $-$46 can transform A1bD into A4bD or A4′bD conformers, respectively, again over potential barriers higher than 20 kJ mol^{-1}. The second low energy basin is related to the A2bD conformer, connected to A4bD through rotation of ϕ_1 from 60 to $\sim$180 over the barrier height of 27 kJ mol^{-1}. Both these regions present deep but rather narrow potential wells. The third basin is centered around the (iso-energetic) A2′bD and IbD conformers. A rotation of ψ_2 from 75 to 6 transforms the γ-turn conformer A2′bD into the β-turn conformer IbD over a low barrier of 6 kJ mol^{-1}. In contrast, the potential barriers between the two types of β-turn structures are relatively high: the transition barrier from IbD to II′bD is 25 kJ mol^{-1} while the inverse barrier is 15 kJ mol^{-1} involving a concerted rotation of ϕ_1 and ψ_1 dihedral angles. Hence, the A2′bD and IbD conformers are confined to a deep and wide potential basin and may interconvert at relatively low temperatures. Similarly, the potential barriers between γ-turn conformer A3bD and β-turn conformer II′bD are also rather low, between 3 and 5 kJ mol^{-1}, because the transitions between γ-turn and β-turn structures do not involve significant atomic rearrangement, and the breaking and re-making of H-bonds occur in a concerted way.

The lower part of Fig. 5 is concerned with the χ_1 and χ_2 dihedral angles related to the puckering motion of the pyrrolidine ring. For the A2′b, Ib, II′b, and A3b conformers, the transition barriers are only between 4 and 9 kJ mol^{-1}, consistent with early force-field calculations[28] as well as X-ray[27] and 2D-NMR experiments.[26] Finally, as shown in the ESI,† the transition barriers between *trans* (A) and *cis* Z-Aib (B) conformations are about 50–80 kJ mol^{-1} in our DFT calculations for the A/B1bD, A/B2bD, A/B2bU, and A/B3aD conformers, which is still slightly lower than for canonical peptide bonds.

D. Site-specific solvent effects on mid-IR spectra

The Z-Aib-Pro-NHMe tripeptide can form clusters with methanol molecules mainly though H-bonding. There are four O-atom sites as possible H-bond acceptors and two N–H sites as possible H-bond donors. Because the peptide backbone conformations are in most cases not significantly altered by the interaction with methanol, the cluster structures listed in Table 2 can be unambiguously assigned to corresponding conformations of the bare peptide, thus allowing for the calculations of unique, conformer specific peptide–methanol binding energies, which are given in the last column of Table 2. The four O-atom acceptor sites, O(11), O(1), O(2), and O(3), are termed **a**, **b**, **c**, **d** and the two N–H donor sites N(1)–H(1) and N(3)–H(3), termed **e**, **f**. When several conformations are possible for one binding site, they are further distinguished by an additional number, as indicated in Fig. 6.

When one methanol is bound to O(11)-atom site **a** as H-bond donor, for the *trans* Z-Aib structure this methanol may easily form an additional H-bond with N–H site **e** nearby

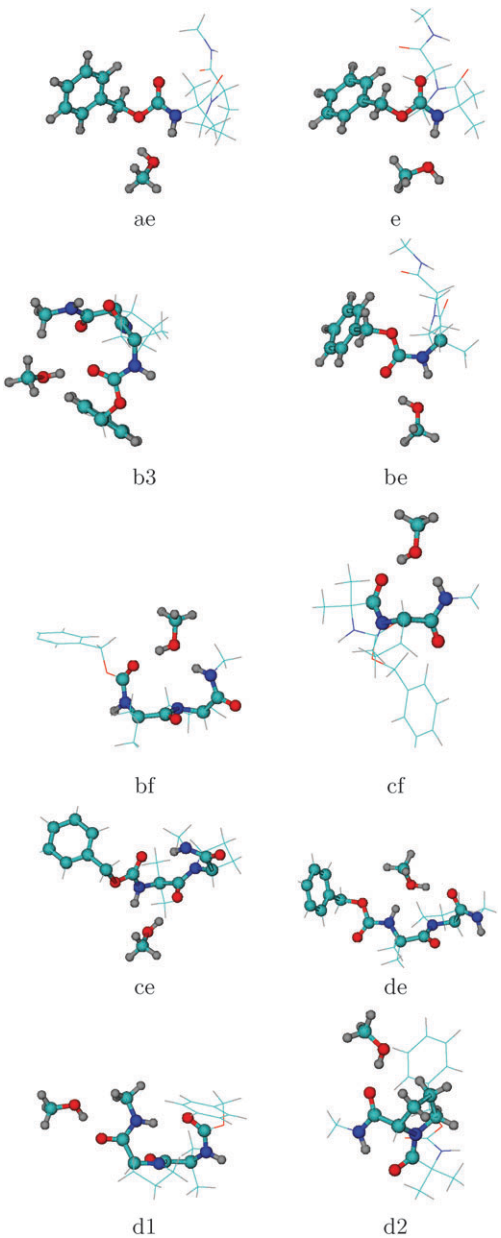

Fig. 6 Minimum energy structures of Z-Aib-Pro-NHMe one-methanol clusters (a, b, c, and d are methanol donor H-bonding sites, while in e and f methanol acts as an acceptor). For values of dihedral angles and binding energies, see the upper part of Table 2.

Table 2 Minimum energy conformations of Z-Aib-Pro-NHMe peptide complexed with one (upper part) and two (lower part) methanol molecules from DFT calculations [B3LYP/6-311++G(d,p)]: dihedral angles (in degrees), and relative energies without and with ZPE corrections and binding energies ΔE (in kJ mol^{-1}). The same nomenclature as in Table 1 is used, with additional indication for the methanol binding sites, see text and Fig. 6 and 9. For more extensive data, see ESI†

Conformation	ϕ_1	ψ_1	ϕ_2	ψ_2	χ_1	χ_2	DFT	DFT + ZPE	ΔE
A1bD_cf	176	172	−75	134	31	−38	0.0	0.5	36.5
A2bD_cf	59	42	−75	135	31	−38	0.4	0.0	39.0
A2′bU_cf	−58	−39	−85	118	−8	28	4.5	4.4	33.7
A2′bU_ae	−55	−38	−80	81	−12	31	9.0	8.9	29.2
A2′bU_d1	−57	−38	−80	79	−12	31	10.9	9.9	27.4
A2′bU_b3	−54	−40	−81	80	−9	29	14.8	13.2	23.0
A2′bU_e	−55	−38	−80	80	−11	30	14.8	13.6	23.5
B2′aU_be	−64	−33	−78	83	−16	33	8.3	8.9	38.7
IaU_bf	−70	−29	−65	−35	−29	38	24.1	22.3	15.4
IbU_d1	−56	−33	−73	−11	−22	36	6.3	4.6	32.4
II′bD_ce	56	−138	−89	9	35	−37	9.6	10.8	38.7
NbU_de	172	−40	−61	134	−26	38	−0.8	−0.4	
A2′bU_cmf	−59	−42	−79	132	−12	30	−6.5	−4.3	71.5
IgU_ae_d2	−56	−33	−71	−14	−23	37	0.0	0.0	66.9
IbU_ae_d2	−56	−33	−71	−14	−23	37	2.5	3.3	63.0
IbU_ae_d1	−56	−33	−73	−11	−22	36	6.3	6.9	59.1
IbU_e_d1	−56	−33	−71	−12	−22	36	10.3	9.8	55.2
IgU_bmf	−69	−36	−68	−38	−25	37	16.9	16.9	50.0

as H-bond acceptor, leading to large binding energy of 29 kJ mol^{-1}, as seen in conformer A2′U_ae. Methanol can also bind to only one of the two adjacent sites **a** or **e** through single H-bonds, as seen, *e.g.*, in conformer A2′U_e, which lowers the binding energies by about 6 kJ mol^{-1}. Note that both sites **a** and **e** are outside the possible γ- and β-turns so that these types of intermolecular H-bonding can coexist with either one of the turn structures. As can be seen from Fig. 7(a), H-bonding from N–H site **e** to methanol blue-shifts the corresponding amide II (#5) and amide III (#9) frequencies by about 50 and 13 cm^{-1}, respectively. Similarly, H-bonding from methanol to site **a** red-shifts the C–O–C stretching mode (#10) to coincide with the C–O stretching mode of methanol while the weak interactions between the methyl group of methanol and O-atom site **a** have no significant effect on the C–O–C stretching frequency.

When one methanol is bound to the O(1)-atom site **b** outside the γ- and β-turn structures, see *e.g.* A2′U_b3 structures, the binding energie are about 23 kJ mol^{-1}. Alternatively, when one methanol is inserted into the β-turn structure and bound to the O-atom site **b** as H-bond donor and to the N–H site **f** as H-bond acceptor (see IaU_bf), the overall methanol binding energy reduces to only 15 kJ mol^{-1} due to breaking of the original β-turn H-bond and further conformational distortion. For a *cis* Z-Aib structure, the O-atom site **b** and the N–H site **e** are adjacent and may bind the same methanol (see *e.g.* B2′U_be), leading to a rather high methanol binding energy of 39 kJ mol^{-1}. As seen from Fig. 7(b), the H-bonding from methanol to the O-atom site **b** causes a red-shift of the corresponding amide I mode (#1) of the Z-Aib peptide bond as indicated by the spectra of A2′U_b3 and B2′U_be. On the other hand, the H-bonding from the N–H site **e** to methanol (see B2′U_be as example) blue shifts the corresponding strong amide III frequency of Z-Aib peptide bond. Insertion of methanol into β-turn structure hardly affect the corresponding amide I, II, III frequencies (see IU_bf) because the H-bonding environment of the involved peptide bonds remains similar.

When one methanol is inserted into the γ-turn structure and bound to the O(2)-atom site **c** as H-bond donor and to the N–H site **f** (see *e.g.* A2′U_cf), the methanol binding energy of about 34 kJ mol^{-1} is larger than for the insertion into a β-turn structure, suggesting that the internal tension for C7-rings (γ-turn) is larger than for C10-rings (β-turn). When methanol is inserted into the γ-turn, the backbone dihedral angle ψ_2 of Pro residue increases by 50–70° as compared with that of the bare tripeptide. As shown in Fig. 7(c), the Aib-Pro amide I frequency (peak #3) is hardly affected but the intensity increases. There is also a blue-shift of 33 cm^{-1} for the Pro-NHMe amide II frequency (peak #4). For type II′ β-turn structures, the O-atom site **c** and the N–H site **e** are adjacent and may together bind a methanol to form a C5 + 2-ring with two new H-bonds, see *e.g.* II′D_ce, leading to a large methanol binding energy of 39 kJ mol^{-1}. The amide I frequencies of the Aib-Pro (peak #3) and the Z-Aib (peak #1) peptide bonds are red-shifted by 36 and 18 cm^{-1}, respectively, now with the later coinciding with the amide I frequency of the Pro-NHMe peptide bond. In addition, the H-bonding from the N–H site **e** to methanol can also blue-shift the corresponding amide II frequency of the Z-Aib peptide bond by 41 cm^{-1}.

When one methanol is bound to the O(3)-atom site **d** outside both γ- and β-turn structures (see IU_d1), the binding energies are about 27–32 kJ mol^{-1}. As seen from Fig. 7(d), this leads to a clear red-shift of 25 cm^{-1} of the amide I frequency of the Pro-NHMe peptide bond with respect to that of the bare tripeptide. Formation of a new structure by an additional H-bonding from the N–H site **e** to the same methanol molecule is also possible (see NU_de as example), leading to a C8 + 2-ring structure replacing γ- and β-turns. Compared to the spectra of the bare tripeptide γ-turn conformer A2′U, the amide I frequency of the Aib-Pro peptide bond is blue-shifted while the amide II of the Pro-NHMe peptide bond is slightly red-shifted due to the opening of the γ-turn structure. Moreover, the new H-bond to the O-atom site **d** only slightly

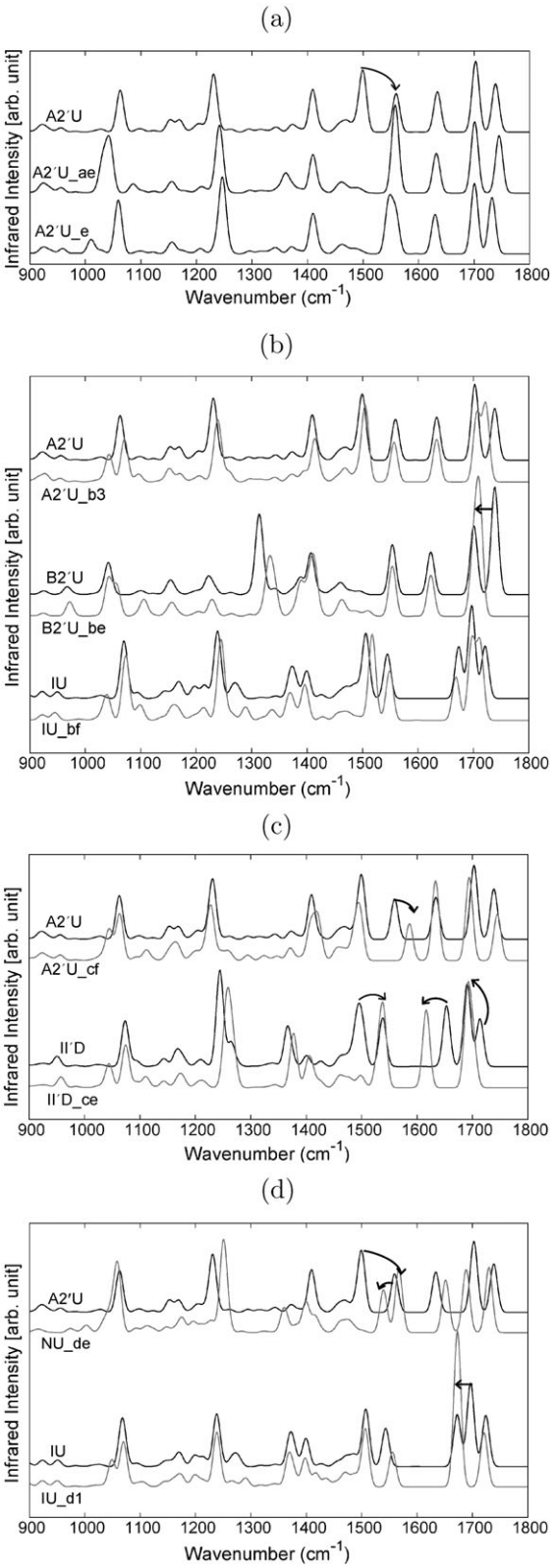

Fig. 7 Effect of methanol H-bonding on mid-IR peptide vibrational spectra. (a) site **e**, also combined with **a**; (b) site **b**, also combined with **e** or **f**; (c) site **c**, also combined with **e** or **f**; (d) site **d**, also combined with **e**.

red-shifts the amide I frequency of the Pro-NHMe peptide bond due to the simultaneous γ-turn opening that can lead to a small blue-shift. The H-bond from the N–H site **e** also blue-shifts the amide II frequency of the Z-Aib peptide bond.

In summary, the H-bonds from methanol to the peptide O-atom sites **b**, **c** and **d** can red-shift the related amide I frequencies, while H-bonds from the N–H sites **e** and **f** to methanol can blue-shift the related amide II and amide III frequencies. This may lead to considerable changes of spectral patterns with respect to those of the bare tripeptide, where the size of the spectral shifts should depend on the strength of H-bonds. Note that the amide II and III bands are strong for the *trans* and *cis* peptide bonds, respectively. Thus, the solvent induced spectral shifts are evident only in the amide II and III regions of the respective *trans* and *cis* peptide bonds.

E. Assignment of observed spectra to clusters with one or two methanols

In the following we shall discuss how the observed spectral shifts of clusters of Z-Aib-Pro-NHMe with one or two methanol molecules can be used to assign the binding sites of methanol, as well as the tripeptide backbone conformation, by comparing computed with experimental spectra, *cf*. Fig. 8(a). Among the simulated spectra of various bare tripeptide conformers, those of the nearly identical γ-turn conformers A2′U and A2U show good agreement with several peaks of the only observed spectrum of the one-methanol cluster. In the most important amide I region, the quantitative agreement for the two peaks around 1740 and 1630 cm^{-1} provides strong evidence of the contribution of a γ-turn structure without H-bonding from methanol to sites **b** and **c**. The dominance of the γ-turn structure with up pyrrolidine

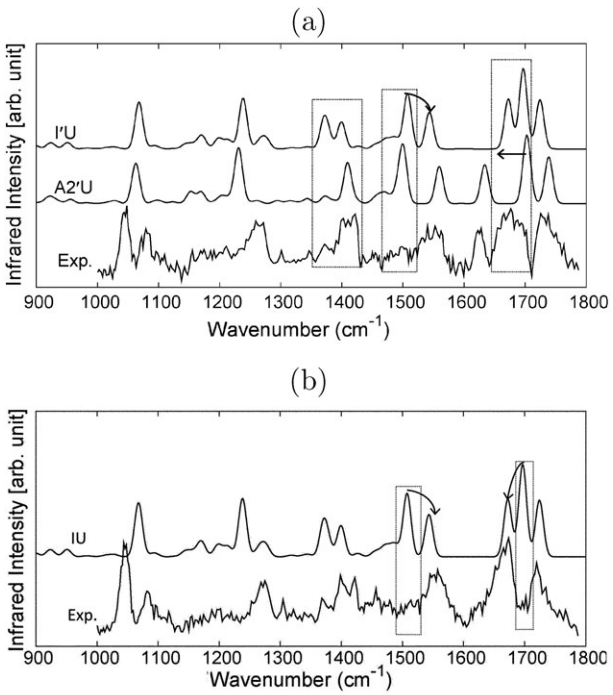

Fig. 8 Comparison between computed mid-IR spectra for selected bare peptide conformations and experimental spectra for Z-Aib-Pro-NHMe micro-solvation clusters with (a) one or (b) two methanol molecules.

puckering rather than β-turn structure is further supported by the good agreement between the A2′U spectrum and the experimental spectrum in the C–N stretching region around 1400 cm^{-1}.

In the amide I region of the experimental spectra, peak #2 around 1680 cm^{-1} is quite broad and slightly red-shifted, most likely due to a mixture of both red-shifted and unshifted amide I frequencies of the Pro-NHMe peptide bond. This suggests that the O-atom site **d** is partially H-bonding to methanol, mainly within the γ-turn rather than β-turn structure as discussed above. Furthermore, in the amide II region of the experimental spectra, peak #5 around 1500 cm^{-1} (Z-Aib peptide bond) almost disappears while peak #4 around 1550 cm^{-1} is broadened, most likely due to a mixture of the blue-shifted Z-Aib and un-shifted Pro-NHMe amide II peaks. This strongly suggests that the N–H site **e** rather than **f** is a binding site for methanol acting as an acceptor. Although methanol can bind either to the O-atom site **d** or the N–H site **e**, the experiments show no evidence for simultaneous binding to both of these sites because such conformers would exhibit neither γ-turn nor β-turn structures (see *e.g.* NU_de as an example) which would lead to qualitatively different spectra. In summary, the experimentally observed conformer of the one-methanol cluster contains mainly γ-turn structures with up-puckering of the pyrrolidine ring (A2′U or A2U) and it must be a mixture with one methanol bound to either site **d** or site **e**. Because the A2′U_e (or A2U_e) conformer is about 6 kJ mol^{-1} less stable than the A2′U_ae (or A2U_ae) conformer, the most likely candidates to match the observed spectrum of one methanol clusters are the A2′U_d (or A2U_d) and A2′U_ae (or A2U_ae) conformers, see Fig. 10(a).

Two methanol molecules can be attached to the Z-Aib-Pro-NHMe tripeptide either as two monomers (*e.g.* IU_ae_d1 and IU_ae_d2) or as a dimer unit (*e.g.* IU_bmf and A2′U_cmf), see Fig. 9. The solvent-induced frequency shifts in the amide vibrations depend mainly on the binding sites of methanol to the tripeptide rather than on H-bonding between two methanol molecules. As seen from Fig. 8(b), the observed spectrum of the two-methanol cluster is consistent only with predicted spectra of β-turn tripeptide conformers. In the most important amide I region, the excellent agreement for the peak around 1725 cm^{-1} together with the enhanced peak around 1670 cm^{-1} provides strong evidence for the existence of a β-turn structure, thereby excluding O-atom sites **b** and **c** as a methanol binding site. In the amide I region of the experimental spectra, peak #2 around 1700 cm^{-1} due to the Pro-NHMe peptide bond disappears while peak #3 around 1670 cm^{-1} is broadened and enhanced. The latter is assigned to a mixture of red-shifted Pro-NHMe and un-shifted Aib-Pro amide I peaks. This strongly suggests the O-site **d** rather than **c** as a methanol binding site. Furthermore, similar to the one-methanol cluster case, the absence of peak #5 around 1500 cm^{-1} and the enhancement of peak #4 around 1550 cm^{-1} in the amide II region of the experimental spectrum indicate that the latter one is a mixture of blue-shifted Z-Aib and un-shifted Pro-NHMe amide II peaks, consistent with the N–H site **e** rather than **f**. Since the β-turn structure can adopt type I or type II′ conformations, the C–N stretching peak around 1400 cm^{-1} in the experiment can provide additional

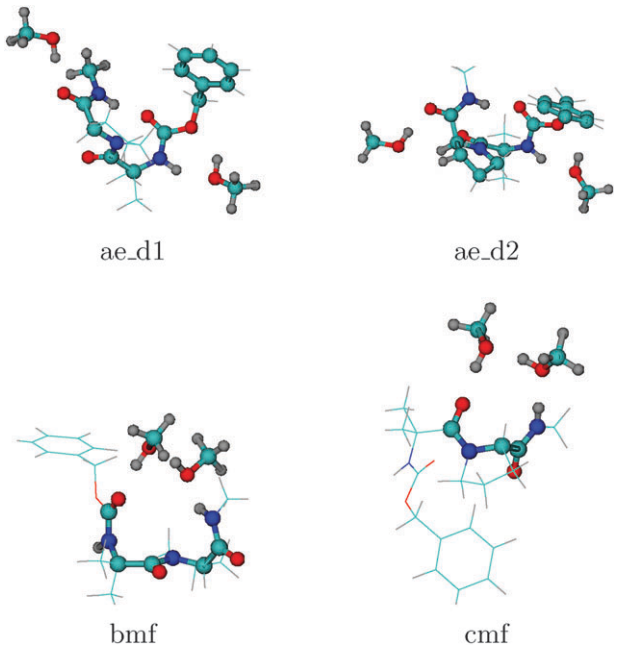

Fig. 9 Minimum energy structures of Z-Aib-Pro-NHMe two-methanol clusters. For nomenclature of methanol binding sites, see Fig. 6. For values of dihedral angles and binding energies, see lower part of Table 2.

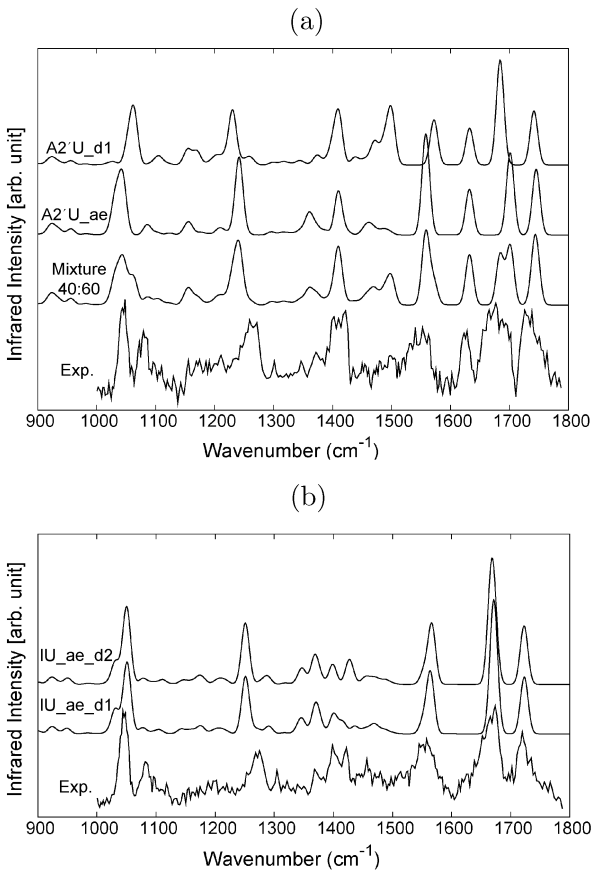

Fig. 10 Simulated and experimental mid-IR spectra for Z-Aib-Pro-NHMe micro-solvation clusters with (a) one and (b) two methanol molecules.

information on the Aib orientation and pyrrolidine ring puckering and thus the β-turn type. The observed spectral pattern with strong peaks around 1400 cm^{-1} is consistent only with the IU conformer; any combinations with type II′ β-turn or down-puckering would lead to strong peaks around 1360 cm^{-1}. The observed spectral patterns in the C–N stretching region around 1400 cm^{-1} are quite similar for all the spectra of the bare peptide and clusters with one and two methanol molecules, suggesting similar Aib orientation and ring puckering for the assigned γ-turn A2′U and β-turn IU conformers, as indeed supported by our calculations. Hence, the most likely candidate for the observed two-methanol cluster should be the IU_ae_d conformer, see Fig. 10(b). Note that the IU_e_d conformer has a similar mid-IR spectrum, but it is about 4 kJ mol^{-1} less stable than the IU_ae_d conformer.

IV. Conclusions

The most favorable sites for methanol binding appear to be the N–H site **e** and O-atom site **d** on the head and tail part of the Z-Aib-Pro-NHMe tripeptide, respectively, which are relatively exposed to methanol solvent to form intermolecular H-bonds. On the other hand, due to the conformational constraints from the Aib and Pro residues, the N–H site **f** tends to form turn structures with the O-atom sites **b** and **c** that are thus screened by the non-polar side-chains. The insertion of methanol molecules into the favorable oligo-peptide turn structures would require substantial deformation of the backbone conformation and involve several reaction steps over potential barriers. For the case of our model Z-Aib-Pro-NHMe tripeptide, the formation of a γ-turn structure appears to be an intrinsic property of the peptide itself, while further H-bonding interactions with methanol molecules (especially on the O-atom site **d**) tend to favor the formation of a β-turn structure, similar to the situation in the crystalline phase[20] and in solutions.[19] In this sense, the one- and two-methanol clusters are bridging the gap between the gas phase and the condensed phase.

Since the observed transition from the γ-turn into the β-turn structure can be induced easily by additional H-bonding interactions with methanol, there should be no significant potential barrier for such transition between secondary structures. In our spectral assignment of the bare peptide and the one-methanol cluster, both the A2′U and A2U conformations of the tripeptide are consistent with the observed γ-turn structure with quite similar potential energy and spectra, but quite different Aib orientation. On the other hand, the observed β-turn structure is assigned to the IU conformation of the tripeptide. Since the former γ-turn structure shows quite similar Aib orientation to that of the observed β-turn structure, low transition barrier and small structural arrangement are required for the transition between them. Indeed, a single-step transition barrier of about 10 kJ mol^{-1} is found for the bare tripeptide and the one-methanol cluster, whereas for the transition between the A2U and the IU conformers of bare tripeptide, a multi-step transition barrier of about 30 kJ mol^{-1} is found. Thus, the observed γ-turn structure of tripeptide is more likely A2′U rather than A2U.

Acknowledgements

Financial support from Deutsche Forschungsgemeinschaft *via* Sonderforschungsbereich 450 is gratefully acknowledged. The simulations were partly carried out at the computing centre (ZEDAT) of the Freie Universitt Berlin. A.M.R. acknowledges the Netherlands Organization for Scientific Research (NWO) for a VENI post-doctoral fellowship.

References

1 L. C. Snoek, R. T. Kroemer and J. P. Simons, *Phys. Chem. Chem. Phys.*, 2002, **4**, 2130, DOI: 10.1039/b200059h.
2 S. J. Xu, M. Nilles and K. H. Bowen, *J. Chem. Phys.*, 2003, **119**, 10696, DOI: 10.1063/1.1620501.
3 P. Carcabal, R. T. Kroemer, L. C. Snoek, J. P. Simons, J. M. Bakker, I. Compagnon, G. Meijer and G. von Helden, *Phys. Chem. Chem. Phys.*, 2004, **6**, 4546, DOI: 10.1039/b411757c.
4 A. Kamariotis, O. V. Boyarkin, S. R. Mercier, R. D. Beck, M. F. Bush, E. R. Williams and T. R. Rizzo, *J. Am. Chem. Soc.*, 2006, **128**, 905, DOI: 10.1021/ja056079v.
5 M. N. Blom, I. Compagnon, N. C. Polfer, G. von Helden, G. Meijer, S. Suhai, B. Paizs and J. Oomens, *J. Phys. Chem. A*, 2007, **111**, 7309, DOI: 10.1021/jp070211r.
6 R. Wu and T. B. McMahon, *J. Am. Chem. Soc.*, 2008, **130**, 3065, DOI: 10.1021/ja076685l.
7 A. Abo-Riziq, B. Crews, L. Grace and M. S. de Vries, *J. Am. Chem. Soc.*, 2005, **127**, 2374, DOI: 10.1021/ja043000y.
8 P. Carcabal, R. A. Jockusch, I. Hünig, L. C. Snoek, R. T. Kroemer, B. G. Davis, D. P. Gamblin, I. Compagnon, J. Oomens and J. P. Simons, *J. Am. Chem. Soc.*, 2005, **127**, 11414, DOI: 10.1021/ja0518575.
9 J. P. Simons, R. A. Jockusch, P. Carcabal, I. Hünig, R. T. Kroemer, N. A. Macleod and L. C. Snoek, *Int. Rev. Phys. Chem.*, 2005, **24**, 489, DOI: 10.1080/01442350500415107.
10 K. Bartl, A. Funk and M. Gerhards, *J. Chem. Phys.*, 2008, **129**, 234306, DOI: 10.1063/1.3037023.
11 C. Tanner, M. Thut, A. Steinlin, C. Manca and S. Leutwyler, *J. Phys. Chem. A*, 2006, **110**, 1758, DOI: 10.1021/jp056151b.
12 A. Budzowski, A. Linden and H. Heimgartner, *Helv. Chim. Acta*, 2008, **91**, 1471, DOI: 10.1002/hlca.200890160.
13 S. Stamm and H. Heimgartner, *Helv. Chim. Acta*, 2006, **89**, 1841, DOI: 10.1002/hlca.200690178.
14 I. Compagnon, J. Oomens, G. Meijer and G. von Helden, *J. Am. Chem. Soc.*, 2006, **128**, 3592, DOI: 10.1021/ja055378h.
15 A. Aubry, D. Bayeul, H. Brückner, N. Schiemann and E. Benedetti, *J. Pept. Sci.*, 1998, **4**, 502.
16 B. Di Blasio, V. Pavone, M. Saviano, A. Lombardi, F. Nastri, C. Pedone, E. Benedetti, M. Crisma, M. Anzolin and C. Toniolo, *J. Am. Chem. Soc.*, 1992, **114**, 6273, DOI: 10.1021/ja00042a001.
17 I. L. Karle, J. L. Flippen-Anderson, K. Uma, H. Balaram and P. Balaram, *Biopolymers*, 1990, **29**, 1433, DOI: 10.1002/bip.360291010.
18 I. L. Karle, J. L. Flippen-Anderson, M. Sukumar and P. Balaram, *Proc. Natl. Acad. Sci. U. S. A.*, 1987, **84**, 5087.
19 C. P. Rao, R. Nagaraj, C. N. R. Rao and P. Balaram, *Biochemistry*, 1980, **19**, 425, DOI: 10.1021/bi00544a004.
20 B. V. V. Prasad, N. Shamala, R. Nagaraj, R. Chandrasekaran and P. Balaram, *Biopolymers*, 1979, **18**, 1635, DOI: 10.1002/bip.1979.360180704.
21 R. Nagaraj, N. Shamala and P. Balaram, *J. Am. Chem. Soc.*, 1979, **101**, 16, DOI: 10.1021/ja00495a003.
22 N. Shamala, R. Nagaraj and P. Balaram, *Biochem. Biophys. Res. Commun.*, 1977, **79**, 292.
23 M. A. Sahai, T. A. K. Kehoe, J. C. P. Koo, D. H. Setiadi, G. A. Chass, B. Viskolcz, B. Penke, E. F. Pai and I. G. Csizmadia, *J. Phys. Chem. A*, 2005, **109**, 2660, DOI: 10.1021/jp040594i.
24 Y. K. Kang, *J. Phys. Chem. B*, 2002, **106**, 2074, DOI: 10.1021/jp013608i.
25 Y. K. Kang, *THEOCHEM*, 2004, **675**, 37, DOI: 10.1016/j.theochem.2003.12.031.
26 M. Cai, Y. Huang, J. Liu and R. Krishnamoorthi, *J. Biomol. NMR*, 1995, **6**, DOI: 10.1007/BF00211775.

27 E. J. Milner-White, L. H. Bell and P. H. Maccallum, *J. Mol. Biol.*, 1992, **228**, 725, DOI: 10.1016/0022-2836(92)90859-I.
28 V. Madison, *Biopolymers*, 1977, **16**, 2671, DOI: 10.1002/bip.1977.360161208.
29 D. F. DeTar and N. P. Luthra, *J. Am. Chem. Soc.*, 1977, **99**, 1232, DOI: 10.1021/ja00446a040.
30 K.-C. Chou, *Anal. Biochem.*, 2000, **286**, 1, DOI: 10.1006/abio.2000.4757.
31 E. Vass, M. Hollósi, F. Besson and R. Buchet, *Chem. Rev.*, 2003, **103**, 1917, DOI: 10.1021/cr000100n.
32 K. Guruprasad and S. Rajkumar, *J. Biosci.*, 2000, **25**, 143.
33 R. H. Page, Y. R. Shen and Y. T. Lee, *J. Chem. Phys.*, 1988, **88**, 4621, DOI: 10.1063/1.453775.
34 W. H. James, E. E. Baquero, V. A. Shubert, S. H. Choi, S. H. Gellman and T. S. Zwier, *J. Am. Chem. Soc.*, 2009, **131**, 6574, DOI: 10.1021/ja901051v.
35 H. Fricke, A. Funk, T. Schrader and M. Gerhards, *J. Am. Chem. Soc.*, 2008, **130**, 4692, DOI: 10.1021/ja076031c.
36 V. Brenner, F. Piuzzi, I. Dimicoli, B. Tardivel and M. Mons, *Angew. Chem., Int. Ed.*, 2007, **46**, 2463, DOI: 10.1002/anie.200604416.
37 E. Gloaguen, F. Pagliarulo, V. Brenner, W. Chin, F. Piuzzi, B. Tardivel and M. Mons, *Phys. Chem. Chem. Phys.*, 2007, **9**, 4491, DOI: 10.1039/b704573e.
38 A. Abo-Riziq, B. O. Crews, M. P. Callahan, L. Grace and M. S. de Vries, *Angew. Chem., Int. Ed.*, 2006, **45**, 5166, DOI: 10.1002/anie.200601516.
39 W. Chin, I. Compagnon, J. P. Dognon, C. Canuel, F. Piuzzi, I. Dimicoli, G. von Helden, G. Meijer and M. Mons, *J. Am. Chem. Soc.*, 2005, **127**, 1388, DOI: 10.1021/ja042860b.
40 W. Chin, M. Mons, J. P. Dognon, F. Piuzzi, B. Tardivel and I. Dimicoli, *Phys. Chem. Chem. Phys.*, 2004, **6**, 2700, DOI: 10.1039/b315470j.
41 I. Hünig and K. Kleinermanns, *Phys. Chem. Chem. Phys.*, 2004, **6**, 2650, DOI: 10.1039/b316295h.
42 B. C. Dian, A. Longarte, S. Mercier, D. A. Evans, D. J. Wales and T. S. Zwier, *J. Chem. Phys.*, 2002, **117**, 10688, DOI: 10.1063/1.1521132.
43 M. Gerhards and C. Unterberg, *Phys. Chem. Chem. Phys.*, 2002, **4**, 1760, DOI: 10.1039/b110029g.
44 H. Fricke, A. Gerlach and M. Gerhards, *Phys. Chem. Chem. Phys.*, 2006, **8**, 1660, DOI: 10.1039/b600154h.
45 J. M. Bakker, C. Plützer, I. Hünig, T. Häber, I. Compagnon, G. von Helden, G. Meijer and K. Kleinermanns, *ChemPhysChem*, 2005, **6**, 120, DOI: 10.1002/cphc.200400345.
46 W. Chin, J. P. Dognon, C. Canuel, F. Piuzzi, I. Dimicoli, M. Mons, I. Compagnon, G. von Helden and G. Meijer, *J. Chem. Phys.*, 2005, **122**, 054317, DOI: 10.1063/1.1839862.
47 W. Chin, M. Mons, J. P. Dognon, R. Mirasol, G. Chass, I. Dimicoli, F. Piuzzi, P. Butz, B. Tardivel and I. Compagnon, *et al.*, *J. Phys. Chem. A*, 2005, **109**, 5281, DOI: 10.1021/jp048037j.
48 J. R. Cable, M. J. Tubergen and D. H. Levy, *J. Am. Chem. Soc.*, 1987, **109**, 6198, DOI: 10.1021/ja00254a057.
49 G. Meijer, M. S. de Vries, H. Hunziker and H. Wendt, *Appl. Phys. B: Photophys. Laser Chem.*, 1990, **51**, 395, DOI: 10.1007/BF00329101.
50 A. M. Rijs, I. Compagnon, J. Oomens, J. S. Hannam, D. A. Leigh and W. J. Buma, *J. Am. Chem. Soc.*, 2009, **131**, 2428, DOI: 10.1021/ja808788c.
51 D. Oepts, A. F. G. Van der Meer and P. W. Van Amersfoort, *Infrared Phys. Technol.*, 1995, **36**, 297, DOI: 10.1016/1350-4495(94)00074-U.
52 A. D. Becke, *J. Chem. Phys.*, 1993, **98**, 5648, DOI: 10.1063/1.464913.
53 C. Lee, W. Yang and R. G. Parr, *Phys. Rev. B: Condens. Matter*, 1988, **37**, 785, DOI: 10.1103/PhysRevB.37.785.
54 M. J. Frisch, G. W. Trucks, H. B. Schlegel, G. E. Scuseria, M. A. Robb, J. R. Cheeseman, J. A. Montgomery, Jr., T. Vreven, K. N. Kudin and J. C. Burant, *et al.*, *GAUSSIAN 03 (Revision C.02)*, Gaussian, Inc., Wallingford, CT, 2004.
55 A. D. McLean and G. S. Chandler, *J. Chem. Phys.*, 1980, **72**, 5639, DOI: 10.1063/1.438980.
56 M. J. Frisch, J. A. Pople and J. S. Binkley, *J. Chem. Phys.*, 1984, **80**, 3265, DOI: 10.1063/1.447079.
57 T. Clark, J. Chandrasekhar, G. W. Spitznagel and P. v. Ragué Schleyer, *J. Comput. Chem.*, 1983, **4**, 294, DOI: 10.1002/jcc.540040303.
58 K. E. Riley, B. T. Op't Holt and K. M. Merz, *J. Chem. Theory Comput.*, 2007, **3**, 407, DOI: 10.1021/ct600185a.
59 B. Santra, A. Michaelides, M. Fuchs, A. Tkatchenko, C. Filippi and M. J. Scheffler, *J. Chem. Phys.*, 2008, **129**, 194111, DOI: 10.1063/1.3012573.
60 J. M. Bakker, L. M. Aleese, G. von Helden and G. Meijer, *Phys. Rev. Lett.*, 2003, **91**, 203003, DOI: 10.1103/PhysRevLett.91.203003.
61 I. Compagnon, J. Oomens, J. Bakker, G. Meijer and G. von Helden, *Phys. Chem. Chem. Phys.*, 2005, **7**, 13, DOI: 10.1039/b417204c.
62 J. Antony, G. von Helden, G. Meijer and B. Schmidt, *J. Chem. Phys.*, 2005, **123**, 014305, DOI: 10.1063/1.1947191.
63 W. Chin, J. P. Dognon, F. Piuzzi, B. Tardivel, I. Dimicoli and M. Mons, *J. Am. Chem. Soc.*, 2005, **127**, 707, DOI: 10.1021/ja045251c.
64 P. N. Lewis, F. A. Momany and H. A. Scheraga, *Biochim. Biophys. Acta, Protein Struct.*, 1973, **303**, 211, DOI: 10.1016/0005-2795(73)90350-4.
65 M. A. Sahai, M. Szöri, B. Viskolcz, E. F. Pai and I. G. Csizmadia, *J. Phys. Chem. A*, 2007, **111**, 8384, DOI: 10.1021/jp074991f.